



**HAL**  
open science

# Data-driven motion compensated SPECT reconstruction for liver radioembolization

Antoine Robert, Simon Rit, Julien Jomier, David Sarrut

## ► To cite this version:

Antoine Robert, Simon Rit, Julien Jomier, David Sarrut. Data-driven motion compensated SPECT reconstruction for liver radioembolization. Fully 3D Image Reconstruction in Radiology and Nuclear Medicine, Jul 2021, Leuven, Belgium. pp.81-84. hal-03376882

**HAL Id: hal-03376882**

**<https://hal.science/hal-03376882>**

Submitted on 13 Oct 2021

**HAL** is a multi-disciplinary open access archive for the deposit and dissemination of scientific research documents, whether they are published or not. The documents may come from teaching and research institutions in France or abroad, or from public or private research centers.

L'archive ouverte pluridisciplinaire **HAL**, est destinée au dépôt et à la diffusion de documents scientifiques de niveau recherche, publiés ou non, émanant des établissements d'enseignement et de recherche français ou étrangers, des laboratoires publics ou privés.

# Data-driven motion compensated SPECT reconstruction for liver radioembolization

Antoine Robert<sup>1,2</sup>, Simon Rit<sup>1</sup>, Julien Jomier<sup>2</sup>, and David Sarrut<sup>1,3</sup>

<sup>1</sup>Univ.Lyon, INSA-Lyon, Université Claude Bernard Lyon 1, UJM-Saint Etienne, CNRS, Inserm, CREATIS UMR 5220, U1206, F-69373, Lyon, France.

<sup>2</sup>Kitware SAS, 6 Cours André Philip, 69100 Villeurbanne

<sup>3</sup>Centre Léon Bérard, 28, rue Laennec, 69373 Lyon Cedex 08, France

**Abstract** The need for quantitative accuracy of single photon emission computed tomography (SPECT) image analysis is increasing with the emergence of targeted radionuclide therapies such as liver radioembolization. Breathing motion is a major issue for quantitation as it leads to misestimation of the tumor activity in the SPECT images. In this paper, we developed a data-driven motion compensated SPECT reconstruction algorithm to account for respiratory motion. A respiratory signal was retrospectively extracted from SPECT list-mode data with the Laplacian Eigenmaps algorithm and used to sort the projections into temporal bins of fixed phase width. A 2D affine motion was then estimated between projections at different phases. The transformation parameters were used to re-bin the list-mode data into one set of compensated projections that was then used to reconstruct a 3D motion-compensated SPECT image using all available events of the list-mode data. The method was evaluated on both simulated and real SPECT acquisitions of liver patients, and compared to respiratory-gated reconstruction. The motion-compensated reconstruction retrieved larger activity in the tumors compared to conventional 3D SPECT reconstruction with a better contrast-to-noise ratio than gated reconstruction.

## 1 Introduction

Single photon emission computed tomography (SPECT) is a key tool for imaging cancer, both for diagnosis and therapeutic purposes. The recent emergence of targeted radionuclide therapies, such as liver radioembolization or neuroendocrine tumors treated with  $^{177}\text{Lu}$ , increased the need for quantitative SPECT analysis, both for pre-treatment planning or per-treatment activity distribution monitoring. One key step in liver radioembolization is the pre-treatment  $^{99\text{m}}\text{Tc}$  SPECT/CT acquisition used to assess lung shunt and extrahepatic uptake. This acquisition can also be used to evaluate the planned dose delivered by therapeutic  $^{90}\text{Y}$  microspheres injected in the liver. The accuracy of this patient-specific treatment planning directly depends on the accuracy of the pre-treatment SPECT images.

Respiratory motion has a major impact on the image quality by blurring the SPECT image. For example, Bastiaannet *et al* [1] showed on simulated data that it may underestimate the SPECT activity in liver tumors. A widely used method to correct for breathing motion in tomography is respiration-gated reconstruction. It consists in using a respiratory signal to sort the measured projections in small temporal respiratory gated frames with minimal motion. Then, the sorted projections are reconstructed phase per phase yielding a series of motion-free volumetric images [2]. This method has proven effective to reduce the blur around moving tumours and improves

the quantification of the tracer concentration. However, the lower photon count in the projection data of each individual time frame compared to conventional reconstruction leads to SPECT images with a poorer signal-to-noise ratio.

Other methods like motion-compensated reconstruction potentially allow to reconstruct images without motion artifacts while using all the available data. This type of method requires the knowledge of the motion of the patient during the whole acquisition. Then, the motion information can be used to combine all individual gated frames into a single motion corrected image either before [3], during [4] or after [5] the reconstruction.

A common method to retrieve the motion vector field is to use a previous 4D image of the same patient, e.g., a 4D CT [4]. However, a 4D image is rarely available in clinical practice and the respiratory motion changes from day to day. Another approach is to estimate the breathing motion field with image registration between the frames of the respiratory-gated PET or SPECT images [3, 6]. In that case, a prior gated reconstruction, which might be time consuming, is needed. Also, additional hardware is often used to get the respiratory signal needed for the gated reconstruction.

One way to avoid the previous reconstruction step is to estimate the movement in projection space. For example, Bruyant *et al* [7] tracked the center of mass of the gated projections to get the motion information. However, this method only assumes rigid motion and might not be suitable for complex tumor deformation.

In this paper, we correct for breathing motion in a conventional SPECT acquisition, without extra hardware or extra image. Affine deformation is estimated between gated projections and accounted for by re-binning list-mode data. The respiratory signal used for gating the projections is extracted from the list-mode data. The method was validated on simulated data and real patient acquisitions and compared to uncorrected and respiratory-gated reconstruction.

## 2 Materials and Methods

We assume a list-mode dataset of a conventional 3D SPECT acquisition, i.e., a list of *events* describing the spatial position, the energy and the time of each photon impinging on the detector for a set of detector positions around the patient.

## 2.1 Breathing signal extraction

A respiratory signal was first estimated using the algorithm described in [8]. The algorithm bins the list-mode data into low-count  $256 \times 256$  pixel projections at a high framerate (200 ms) and uses Laplacian Eigenmaps to reduce the dimensionality to a 1D breathing signal sampled at 200 ms. The breathing phase was computed by assuming linearity from 0% to 100% between two consecutive end-inhale positions.

## 2.2 Motion estimation

The projections were then gated using the breathing phase. Projections were sorted into temporal bins sampling the breathing cycle regularly, eight for patient acquisitions and twenty for simulated data. The projections were acquired with a dual-head SPECT system (section 2.5), thus acquiring two opposite projections per gantry angle. For motion estimation, one of the two projections was laterally flipped and added to the other to improve the signal to noise ratio during the registration.

A reference bin was chosen and the other projection bins were registered to it using the Elastix image registration package [9]. Registration computed a 2D affine transformation (6 degrees of freedom) using the correlation coefficient as similarity measure and adaptive stochastic gradient descent for the optimisation. The resulting transformations were then applied to the list-mode data to bin a set of motion-compensated projections, keeping the two opposite projections separated. This step compensates the *apparent* 2D projective motion in the projections.

For each acquisition, we generated one set of compensated projections corresponding to the end-inhale position. This bin was chosen because it minimizes the attenuation correction error made by the use of a 3D attenuation map for liver tumors located close to the lungs.

## 2.3 SPECT reconstruction

All volumes were reconstructed using the Reconstruction Toolkit (RTK) [10]. The projections were reconstructed with 20 iterations and 4 subsets into a  $128^3$  voxel matrix (voxel size 4.42 mm), using the OSEM algorithm with a quadratic penalization. All the reconstructions included scatter and attenuation correction. For the attenuation correction, the 3D CT image acquired by the SPECT/CT system (section 2.5) was used.

For each dataset, we reconstructed one conventional 3D image with no motion compensation, one respiratory-gated 4D image and one motion-compensated 3D image with the proposed method. In addition, for the simulation dataset, reference 3D images were reconstructed with the patient static at end-inhale.

## 2.4 SPECT simulation

The SPECT acquisition of a breathing patient was simulated with the Monte Carlo software Gate [11]. The simulated SPECT scanner was the same as the one of the patient acquisitions (section 2.5). Patient motion over a breathing cycle was estimated on the 4D CT image of a thoracic patient. The end-exhale phase was used as reference and registered to each of the nine other phases using 3D deformable image registration. The liver was delineated on the CT image of the reference phase and a spheroid activity source of 20 mm radius was positioned in the liver with of 1:9 ratio between the activity in the tumor and the liver activity in the background. Deformation vector fields were interpolated between consecutive frames to obtain 20 frames which were applied to the reference frame of the 4D CT and the activity sources (tumor and background). The resulting 20 positions in the respiratory motion were simulated individually. At the end of the simulation, the twenty list-mode files were gathered into a single list-mode file according to the input respiratory signal to mimic the acquisition of a breathing patient with a continuous rotation.

## 2.5 Patient acquisitions

The patient datasets were acquired with the dual-head General Electric Discovery NM/CT 670 of the Léon Bérard cancer center equipped with the Low Energy High Resolution (LEHR) collimator. Sixty projections were acquired over  $360^\circ$ , each with  $128 \times 128$  pixels, 4.42 mm isotropic spacing and an acquisition time of 25 s. Patient acquisitions used for this study came from the pre-treatment imaging of liver radioembolization procedure. This step consists in injecting around 350 MBq of  $^{99m}\text{Tc}$  macro aggregated albumin (MAA) inside the liver to assess lung shunt and extrahepatic uptake. Twelve distinct patients were included in this study. One patient was scanned three times but the results were analyzed separately, yielding fourteen patient samples.

## 2.6 Image analysis

On each reconstructed volume, a volume of interested (VOI) was delineated. For the simulations, the VOI of the reference 3D SPECT image (with no motion), of the motion-compensated reconstructions and of each frame of the reconstructed 4D image was the known tumor delineation at the respective position in the breathing cycle. The VOI of the blurred 3D image was the union of the 20 tumor positions. For the patient acquisitions, a fixed threshold at 42% of the maximum value was used to define the VOI [12].

The activity was evaluated by computing the mean activity  $A$  in the VOI. The activity recovery was defined as follows:

$$\Delta A = \frac{A_{\text{evaluated}} - A_{\text{ref}}}{A_{\text{ref}}} \times 100 \quad (1)$$

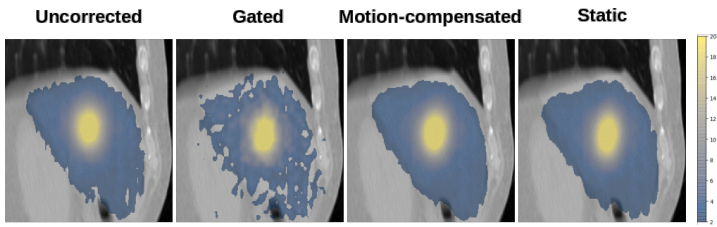


**Figure 1:** Sagittal slices of the images reconstructed from the SPECT simulation. The gated, motion-compensated and static images are images of the end-inhale position.

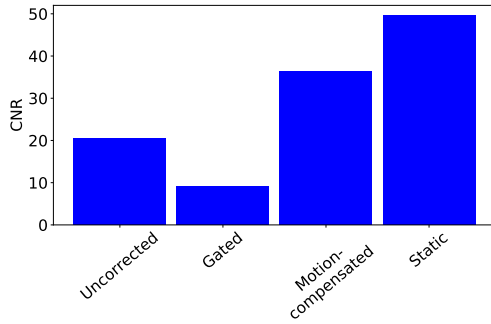


**Figure 2:** Contrast-to-noise ratio for the different reconstructions of the SPECT simulation.

where  $A_{\text{evaluated}}$  was the mean activity in the VOI of either the gated, motion-compensated or blurred reconstruction and  $A_{\text{ref}}$  the one in the reference image. The reference was the reconstruction with no motion for the simulation and the blurred reconstruction for the patient acquisition.

The contrast-to-noise ratio (CNR) was computed for each reconstruction as follows:

$$\text{CNR} = \frac{\mu_1 - \mu_2}{\sigma_2} \quad (2)$$

where  $\mu_1$  is the mean activity in the VOI,  $\mu_2$  the one in the background and  $\sigma_2$  the corresponding standard deviation.

The amplitude of the tumor motion was also measured in each acquisition by tracking the center of mass in the respiratory-gated reconstruction.

### 3 Results

#### 3.1 Simulations

Sagittal slices of the images reconstructed from simulated data are shown in Figure 1. Motion-compensated reconstruction visually improved image quality compared to the gated or the blurred reconstructions.

This visual observation was quantitatively confirmed by the CNR value (Figure 2), which was higher for the motion-compensated reconstruction than the reconstruction without motion correction and the gated reconstruction and closer to the reference.

The mean activity in the tumor of the blurred 3D reconstruction was 24% lower than the reference. The gated and the

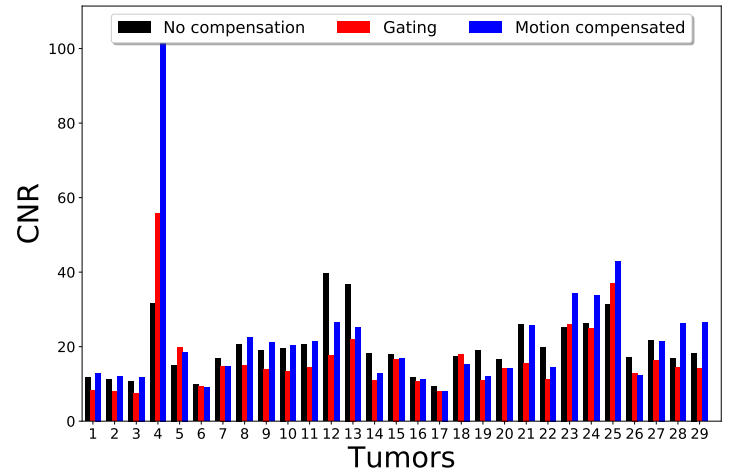


**Figure 3:** Contrast-to-noise ratio for the 29 tumors segmented on the patient reconstructions.

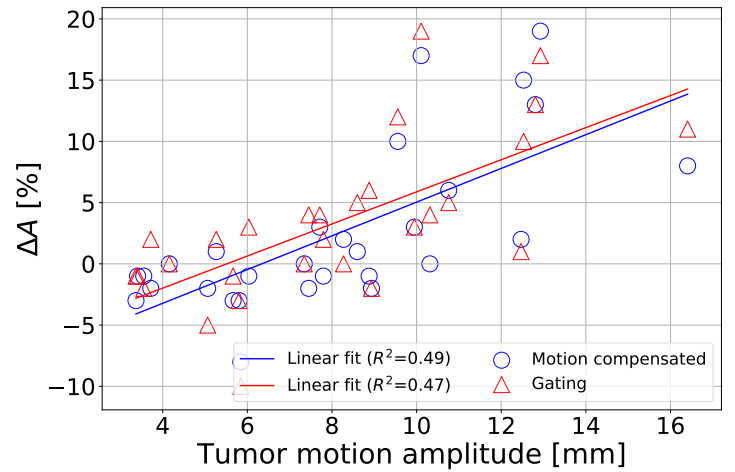


**Figure 4:** Activity recovery  $\Delta A$  for the gated and motion-compensated images of the patient acquisitions at end-inhale. The blurred image was used as reference.

motion-compensated reconstructions were closer to the reference: 1% below and 2% above, respectively.

#### 3.1.1 Patients

Patient evaluation included 29 tumors in 20 SPECT acquisitions of different patients. The average motion amplitude was 8.1 mm with a 3.4–16.4 mm range. The CNR value is given in Figure 3. On average, the CNR in the motion-compensated SPECT image was 31.1% and 8.2% higher than the one obtained with the gated and the blurred SPECT images, respectively. The maximum gains were 90.1% and 234% compared to the uncorrected and the gated reconstructions.

The activity recovery  $\Delta A$  was 3.4% on average with a -10%–19% range for the gated reconstruction. The average value was 2.3% for the motion-compensated reconstruction and the value range between -8% and 19% (Figure 4).

## 4 Discussion

The proposed motion-compensated reconstruction was applied to simulated and real liver radioembolization pretreatment  $^{99m}\text{Tc}$  SPECT acquisitions. The method is fully data-driven and does not require any extra-hardware or other image than the conventional 3D SPECT list-mode data.

The motion-compensated reconstruction recovered larger activity value in the tumor compared to the reconstruction without compensation. On the simulation, the activity recovery  $\Delta A$  was closer to the reference 3D reconstruction obtained from a static simulation.

For the patient acquisition, the average increase was 2.3% compared to the uncorrected reconstruction. For five tumors, this value was above 10%. The activity recovery was slightly correlated to the tumor motion amplitude (fig. 4). Therefore, for tumors with substantial motion, the motion-compensated reconstruction should help to improve the predictive dosimetry for  $^{90}\text{Y}$  radioembolization, leading to more accurate patient-specific treatment planning. However, further studies are needed to assess the real impact on the predictive dosimetry, e.g. studying the impact of the method on the quantification of the tumor-to-normal liver ratio or the lung shunt fraction.

The use of a 3D attenuation map to perform the attenuation correction of the motion-compensated reconstruction might lead to mismatch between the attenuation map and the emission map. This can result in under- or over-estimation of the activity recovery depending on the tumor location. The most critical position is near the border between the liver and the lung, which have very different attenuation coefficients. In that case, part of the tumor can match the lung position in the attenuation map when reconstructed at end-exhale, whereas at end-inhale, most of the tumor is in the liver. In this study, we chose to reconstruct the motion-compensated images at end-inhale to mitigate this effect.

The activity recovery obtained with motion-compensated reconstruction was in the same range as the one obtained with respiratory-gated reconstruction. However, motion compensation improved the CNR with respect to gated reconstruction. Higher CNR could improve the detection of small tumors or regions with low uptake ratios, thus improving the diagnostic. In this study, we only considered tumors in the liver but the method can be easily adapted to other organs. However, it might be limited by the estimation of motion in the projections since two tumors might overlap but move differently in these images [3].

## 5 Conclusion

We have developed a fully data-driven motion-compensated SPECT reconstruction and evaluated it in the context of liver radioembolization. The method was compared to a respiratory-gated reconstruction in terms of activity recovery and CNR. The motion compensation recovered larger

activity in the tumor compared to conventional 3D SPECT reconstruction with higher CNR than respiratory-gated reconstruction, which should eventually improve the treatment planning of liver radioembolization.

## References

- [1] R. Bastiaannet, M. A. Viergever, and H. W.A. M. de Jong. "Impact of Respiratory Motion and Acquisition Settings on SPECT Liver Dosimetry for Radioembolization". eng. *Medical Physics* 44.10 (Oct. 2017), pp. 5270–5279. DOI: [10.1002/mp.12483](https://doi.org/10.1002/mp.12483).
- [2] L. Boucher, S. Rodrigue, R. Lecomte, et al. "Respiratory Gating for 3-Dimensional PET of the Thorax: Feasibility and Initial Results". eng. *Journal of Nuclear Medicine: Official Publication, Society of Nuclear Medicine* 45.2 (Feb. 2004), pp. 214–219.
- [3] F. Lamare, T. Cresson, J. Savean, et al. "Respiratory Motion Correction for PET Oncology Applications Using Affine Transformation of List Mode Data". eng. *Physics in Medicine and Biology* 52.1 (Jan. 2007), pp. 121–140. DOI: [10.1088/0031-9155/52/1/009](https://doi.org/10.1088/0031-9155/52/1/009).
- [4] F. Qiao, T. Pan, J. W. Clark, et al. "A Motion-Incorporated Reconstruction Method for Gated PET Studies". *Physics in Medicine and Biology* 51.15 (Aug. 2006), pp. 3769–3783. DOI: [10.1088/0031-9155/51/15/012](https://doi.org/10.1088/0031-9155/51/15/012).
- [5] Wenjia Bai and M. Brady. "Regularized B-Spline Deformable Registration for Respiratory Motion Correction in PET Images". *2008 IEEE Nuclear Science Symposium Conference Record*. Oct. 2008, pp. 3702–3708. DOI: [10.1109/NSSMIC.2008.4774124](https://doi.org/10.1109/NSSMIC.2008.4774124).
- [6] G. Klein, R. Reutter, and R. Huesman. "Four-Dimensional Affine Registration Models for Respiratory-Gated PET". *IEEE Transactions on Nuclear Science* 48.3 (June 2001), pp. 756–760. DOI: [10.1109/23.940159](https://doi.org/10.1109/23.940159).
- [7] P. P. Bruyant, M. A. King, and P. H. Pretorius. "Correction of the Respiratory Motion of the Heart by Tracking of the Center of Mass of Thresholded Projections: A Simulation Study Using the Dynamic MCAT Phantom". *IEEE Transactions on Nuclear Science* 49.5 (Oct. 2002), pp. 2159–2166. DOI: [10.1109/TNS.2002.803678](https://doi.org/10.1109/TNS.2002.803678).
- [8] J. C. Sanders, P. Ritt, T. Kuwert, et al. "Fully Automated Data-Driven Respiratory Signal Extraction From SPECT Images Using Laplacian Eigenmaps". eng. *IEEE transactions on medical imaging* 35.11 (Nov. 2016), pp. 2425–2435. DOI: [10.1109/TMI.2016.2576899](https://doi.org/10.1109/TMI.2016.2576899).
- [9] S. Klein, M. Staring, K. Murphy, et al. "Elastix: A Toolbox for Intensity-Based Medical Image Registration". eng. *IEEE transactions on medical imaging* 29.1 (Jan. 2010), pp. 196–205. DOI: [10.1109/TMI.2009.2035616](https://doi.org/10.1109/TMI.2009.2035616).
- [10] S Rit, M Vila Oliva, S Brousmiche, et al. "The Reconstruction Toolkit (RTK), an Open-Source Cone-Beam CT Reconstruction Toolkit Based on the Insight Toolkit (ITK)". *Journal of Physics: Conference Series* 489 (Mar. 2014), p. 012079. DOI: [10.1088/1742-6596/489/1/012079](https://doi.org/10.1088/1742-6596/489/1/012079).
- [11] D. Sarrut, M. Bardiès, N. Bousson, et al. "A Review of the Use and Potential of the GATE Monte Carlo Simulation Code for Radiation Therapy and Dosimetry Applications". eng. *Medical Physics* 41.6 (June 2014), p. 064301. DOI: [10.1118/1.4871617](https://doi.org/10.1118/1.4871617).
- [12] Y. E. Erdi, B. W. Wessels, M. H. Loew, et al. "Threshold Estimation in Single Photon Emission Computed Tomography and Planar Imaging for Clinical Radioimmunotherapy". en. *Cancer Research* 55.23 Supplement (Dec. 1995), 5823s–5826s.